Journal of Medicinal Chemistry

Article

pubs.acs.org/jmc

Crystal Structure of Human Aurora B in Complex with INCENP and VX-680

Jonathan M. Elkins,*[,†] Stefano Santaguida,[‡,⊥] Andrea Musacchio,[‡,§,∥] and Stefan Knapp[†]

[†]Nuffield Department of Clinical Medicine, Structural Genomics Consortium, University of Oxford, Old Road Campus Research Building, Roosevelt Drive, Oxford, OX3 7DQ, United Kingdom

[‡]Department of Experimental Oncology, European Institute of Oncology, Via Adamello 16, 20139 Milan, Italy

[§]Department of Mechanistic Cell Biology, Max Planck Institute of Molecular Physiology, Otto-Hahn-Straße 11, 44227 Dortmund, Germany

[∥]Centre for Medical Biotechnology, Faculty of Biology, University Duisburg-Essen, Universitätsstrasse, 45141 Essen, Germany

Supporting Information

ABSTRACT: We present the structure of the human Aurora B kinase domain in complex with the C-terminal Aurora-binding region of human INCENP and the Aurora kinase inhibitor VX-680. The structure unexpectedly reveals a dimeric arrangement of the Aurora B:INCENP complex, which was confirmed to exist in solution by analytical ultracentrifugation. The dimerization involves a domain swap of the activation loop, resulting in a different conformation of the DFG motif as compared to that seen in other kinase complexes with VX-680. The binding of INCENP differs significantly from that seen in the *Xenopus laevis* Aurora B:INCENP complex currently used as a model for structure-based design for this important oncology target.

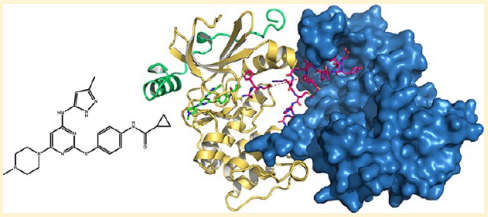

INTRODUCTION

Mammals express three Aurora kinases, Aurora A, Aurora B, and Aurora C, encoded by the genes AURKA, AURKB, and AURKC. Aurora C expression is mainly restricted to testis, where it functions during meiosis, whereas Aurora A and B play key functions regulating mitosis. Aurora A is localized to the centrosome and spindle poles, where it drives centrosome maturation, separation, and bipolar spindle assembly. Aurora B is the central component of the chromosomal passenger complex (CPC) that also contains the inner centromere protein (INCENP), borealin, and survivin. These non-enzymatic components of the CPC play a key role in regulating kinase activity and localization.[1,2] The Aurora kinases are related to the AGC (protein kinase A, protein kinase G, and protein kinase C) branch of protein kinases.[3] Part of the activation mechanism for most AGC kinases is mediated by binding of the phosphorylated C-terminal "hydrophobic motif", FXXF(T/S)F, to the N-terminal lobe of the kinase catalytic domain. However, Aurora kinases lack canonical C-terminal hydrophobic motifs and are activated in trans through binding of regulatory proteins to their N-terminal lobe. Aurora A is activated through interaction with TPX2. For Aurora B and Aurora C, the C-terminal section of the INCENP protein (the "IN-box") performs a similar regulatory function.[4]

The structure of human Aurora A has been determined both without TPX2[5,6] and in complex with TPX2.[7] The structure of Aurora B has previously been determined from *Xenopus laevis*, in complex with INCENP and the Aurora B inhibitor hesperadin[8] as well as other inhibitors.[9−12] Human Aurora B is 80% identical to *X. laevis* Aurora B over the kinase domain (55−344) and 72% identical to human Aurora A over the kinase domain. Human INCENP is 50% identical to *X. laevis* INCENP over the region 835−903 that is involved in binding to Aurora B.

Aurora A phosphorylated on the activation loop in the absence of TPX2 has been observed in both active[6] and inactive conformations.[5,6] Aurora A has been cocrystallized together with **1** (VX-680, Figure 1) in the presence of TPX2, which caused binding to an active kinase conformation,[13] and also in the absence of TPX2, which caused **1** to bind to an inactive conformation of the kinase domain,[14] although this latter structure is not yet available in the Protein Data Bank.

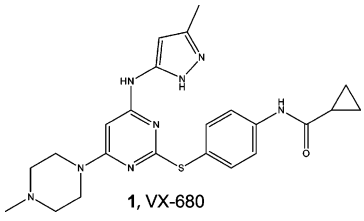

Figure 1. Chemical structure of compound **1** (VX-680).

Aurora B is activated by phosphorylation of both Aurora B and INCENP. First, phosphorylation of INCENP at the TSS

Received: June 25, 2012
Published: August 27, 2012

motif of the C-terminal IN-box region, which can be performed by Aurora B itself, is important for full activity.[8,15] Second, autophosphorylation on the activation loop of Aurora B (for human Aurora B at Thr232) produces the active kinase.[8] A recent study showed that phosphorylation on Ser331 of Aurora B by Chk1 was essential for phosphorylation of the TSS motif of INCENP and also for full activation of Aurora B.[16]

Although most genetic alterations identified in cancer involve the Aurora A locus, high expression levels of Aurora B have been detected and associated with poor prognosis in glioblastoma, ovarian carcinoma, and hepatocellular carcinoma. Inhibition of Aurora B leads to failure to biorientate chromosomes and massive polyploidization. As a result of the induced chromosomal defects, both p53-proficient and p53-deficient cells undergo apoptosis. Aurora B has therefore become an extensively pursued anticancer target,[17] and many Aurora inhibitors have been developed, including recently some isoform-specific inhibitors.[18−22] The Aurora kinase inhibitors (second generation type 2 inhibitors) such as **1**[23] have considerable antitumor activity. Compound **1** also inhibits some other kinases, notably the tyrosine kinase ABL, and crystal structures have been solved for **1** bound to ABL1[24] and ABL2.[25]

To provide a model for structure-based design and to gain insight into the molecular mechanism of human Aurora B activation, we determined the structure of human Aurora B kinase domain, in complex with the C-terminal IN-box section of human INCENP (residues 835−903) and the type II inhibitor **1** (Figure 1).

RESULTS

Structure Determination. We began structural studies on human Aurora B by preparing a set of constructs spanning different ranges of the gene, all of which included the kinase domain, for overexpression in *Escherichia coli*. From this set, three constructs (55−344, 65−344, and 70−344) expressed large amounts of soluble protein. However, all of these proteins precipitated shortly after Ni^{2+}-affinity purification. Therefore, a bacterial expression construct for the C-terminal part of human INCENP was prepared, spanning residues 835−903, which is the Aurora-binding region. This expression construct contained a glutathione-*S*-transferase purification tag to enable sequential affinity purification of the heterodimeric Aurora B:INCENP complex by sequential Ni^{2+}-affinity followed by glutathione sepharose affinity chromatography. The two proteins were expressed separately, and the cells were mixed before lysis and subsequent protein purification. The Aurora B protein was monophosphorylated according to electrospray ionization mass spectrometry (data not shown). Using this purified protein, we were able to cocrystallize the Aurora B INCENP heterodimer in complex with the type II inhibitor **1** and determine the structure to a resolution of 2.75 Å (Table 1).

Structure of Human Aurora B. As expected from the primary sequence similarities, the overall structure of human Aurora B resembles the structures of *X. laevis* Aurora B and human Aurora A, with the exception of the conformation of the activation loop (Figure 2). Unexpectedly, a domain swap was observed; part of the kinase activation loop was exchanged between two Aurora B molecules in the crystal lattice, resulting in similar binding of the activation loop against the C-terminal lobe of the kinase but different conformations around the DFG (Asp-Phe-Gly) motif at the start of the activation loop (Figure 3A). Although this is a feature that has been observed before in kinase crystal structures,[26−28] to our knowledge, this is the first time it has been observed in an Aurora kinase structure. Activation loop exchange has been suggested as an activation mechanism for kinases that autoactivate on nonconsensus binding sites in their activation segment. In the Aurora B:INCENP complex, the activation segment is disordered after the DFG motif, including the phosphorylation site Thr232. The C-terminal part of the activation segment is dislodged from the lower lobe and interacts with a deep groove generated by the displaced activation segment in the interacting protomer. Overall, there is a buried surface area of interaction of 3460 $Å^2$, and the segment is anchored mainly by aromatic and hydrophobic interactions of Y239, L237, Pro242, and I245 (Figure 3C,D).

Table 1. Data Collection and Refinement Statistics

unit cell [*a*, *b*, and *c* (Å); *α*, *β*, and *γ* (deg)]	80.1, 80.1, 92.5, 90.0, 90.0, 120.0
space group	$P3_121$
no. of molecules/asu	1
data collection	
resolution range[a] (Å)	19.58−2.75 (2.90−2.75)
completeness[a] (%)	99.7 (100.0)
multiplicity[a]	11.8 (7.0)
R_{merge}[a] (%)	0.082 (0.936)
$\langle I/\sigma(I)\rangle$[a]	22.6 (2.0)
refinement	
R factor (%)	20.5
R_{free} (%)	26.4
rmsd bond length (Å) [angle (°)]	0.008 (1.22)
PDB ID	4AF3

[a]Values in parentheses are for the highest resolution shell.

The electron density unambiguously favored the loop-exchanged arrangement over the alternative model of a conventional arrangement (Figure 3B). The residues at the point of the domain swap form more favorable interactions than they would have in the case of a nonexchanged arrangement (Figure 3B). In particular, there is a favorable hydrophobic packing of the side chain of Met249 with Met244 and a favorable interaction of His250 with His198.

Met249, which is important for the formation of the domain-swapped form, is not conserved in *X. laevis* Aurora B, which has Thr265 instead. Apart from one conservative substitution of an arginine for a lysine, this is the only difference in the activation loop between the human and *X. laevis* enzymes, which is one of the most highly conserved regions in the whole protein. Given the very favorable nature of the hydrophobic packing of the Met249 side chain, it may be that this single amino acid difference is responsible for the observation of a domain swapped dimeric form of Aurora B only for crystals of the human orthologue.

In this domain-swapped arrangement, part of the activation loop packs against the outside of helix *α*C, which is important for the activity and regulation of protein kinases. Whether this arrangement has any effect on the activity or regulation of human Aurora B kinase is an open question, but it may be partly responsible for the outward movement of *α*C relative to the structures of *X. laevis* Aurora B with **1** and ABL1/2 with **1** (discussed below).

Oligomeric State Distribution. After observing the activation loop in the domain swapped conformation, to see if the dimeric state was also observed in solution, we analyzed the oligomeric state of the complex by analytical ultra-

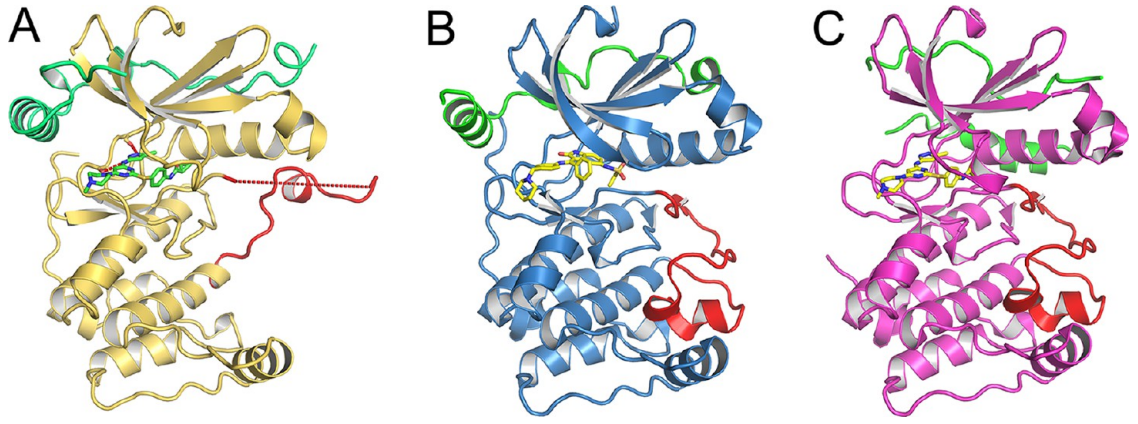

Figure 2. Overview of human Aurora B kinase as compared to *X. laevis* Aurora B and human Aurora A. (A) Human Aurora B with INCENP colored green and the activation loop colored red. (B) *X. laevis* Aurora B complex with Hesperadin (PDB ID: 2BFY),[8] with INCENP colored green and the activation loop colored red. (C) Human Aurora A complex with **1** (PDB ID: 3E5A),[13] with TPX2 colored green and the activation loop colored red.

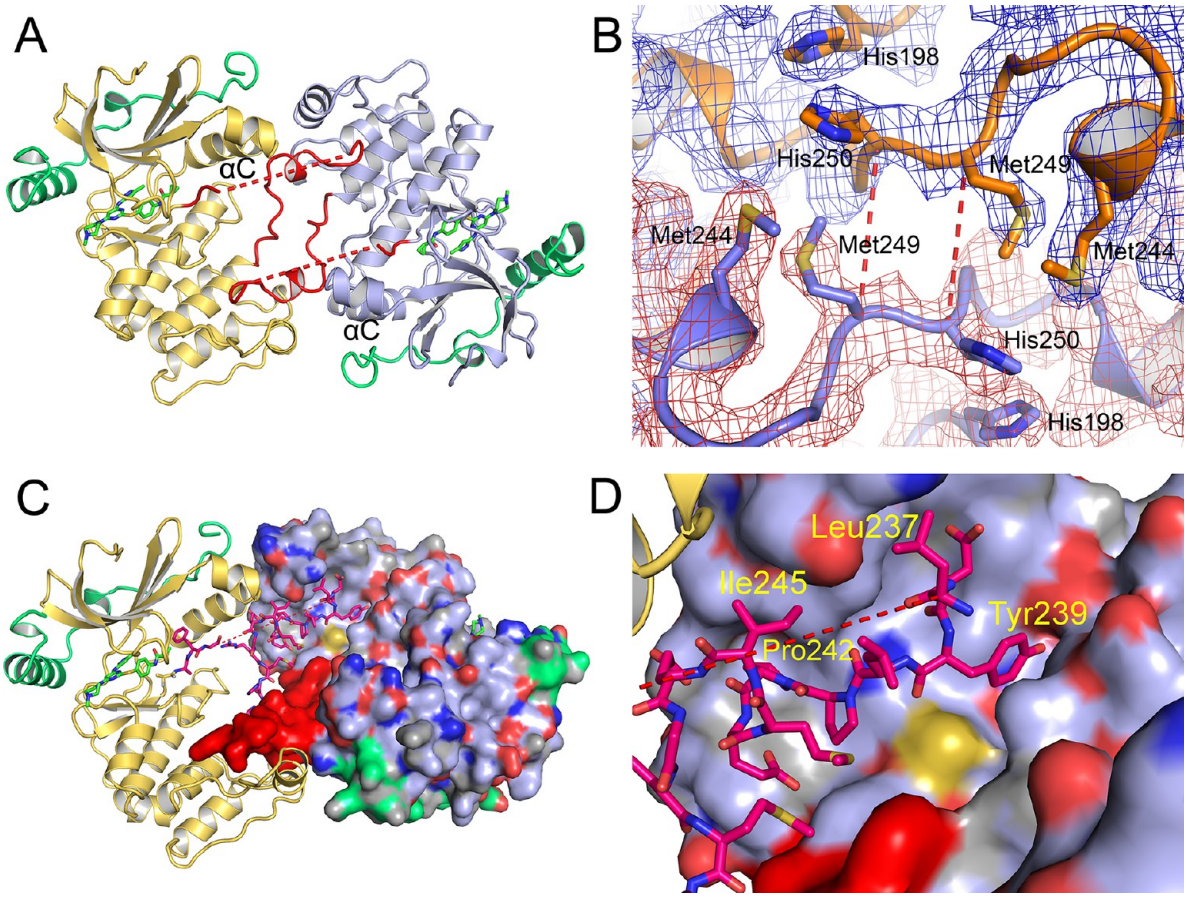

Figure 3. Activation loop exchange of Aurora B kinase. (A) The two Aurora B molecules in the dimer are colored in yellow and blue, INCENP is green, and the activation loops are colored red with dashed lines to indicate where the disordered residues would form a connection. Part of the activation loop packs against the αC helix. (B) The electron density at the cross-over point for the domain swap. The two molecules of Aurora B are colored in orange and blue. The dashed lines in red indicate the connections that would be made between Met249 and His250 in the absence of a domain swap. (C) As in panel A but with one Aurora B:INCENP molecule displayed as a surface, showing the binding of the activation loop in the dimeric arrangement. (D) The activation loop residues involved in the binding.

centrifugation (AUC). A sedimentation velocity experiment showed the presence of both monomer and dimer, with the majority of the sample being dimeric (Figure 4). As the monomer and dimer had different frictional ratios (f/f_0), the data were modeled as a dual distribution of s and f/f_0.[29] The sedimentation velocity analysis gave molecular weights of 43307 and 81882 for the two species present, which compared well with the expected values of 41849 and 83680 for monomer and dimer based on the protein sequences. The frictional ratio for the dimeric species was higher at 2.09, as compared to 1.94 for the monomeric species, corresponding to a less spherical dimeric arrangement. Integration of the distribution resulted in values of 54% dimer and 31% monomer, plus 11% of a species

dx.doi.org/10.1021/jm3008954 | J. Med. Chem. 2012, 55, 7841−7848

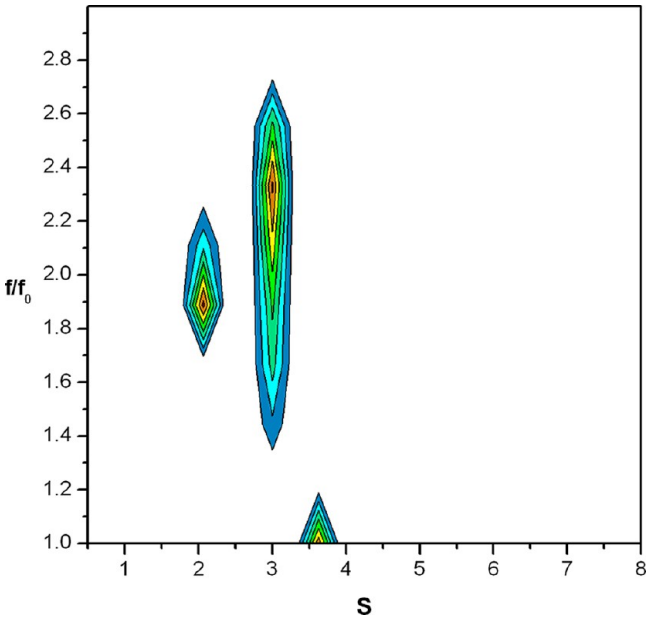

Figure 4. Sedimentation velocity analysis of AuroraB:INCENP, showing a 2D plot of f/f_0 on the *Y*-axis and *s* on the *X*-axis. The smaller and larger peaks correspond to monomeric and dimeric AuroraB:INCENP, respectively. Peak height is indicated by color on a scale from blue to red (strongest).

of approximately 49 kDa with a significantly lower frictional ratio than the peaks assigned as monomer and dimer.

Interface between Aurora B and INCENP. The C-terminal part of INCENP, the IN-box, wraps around the N-terminal lobe of the Aurora B kinase domain in a manner similar to that seen previously with the *X. laevis* orthologue. The two proteins are 50% identical over the region used in the construct for crystallization (835−903) (Figure 5A). However, although the binding of the N-terminal part of the N-box (residues 842−863, "site 1") closely resembles that of the *X. laevis* Aurora B INCENP structure (Figure 5B), the C-terminal part (residues 868−881, "site 2") is mostly different, with a substantial variation in the backbone conformation of the INCENP residues at site 2 (Figure 5C). At site 1, the INCENP backbone adopts the same α-helical arrangement, with the only significant differences in binding being for the nonconserved residues Ile856 of INCENP and Leu210 of Aurora B, which are Arg812 and Tyr228 in the *X. laevis* orthologue. The human complex therefore has a hydrophobic interaction at this point in place of the hydrogen bond between the Tyr and the Arg side chains in *X. laevis*.

At site 2, the INCENP backbone adopts a different conformation with only the binding of the very C-terminal Phe881 conserved (Figure 5C). Furthermore, the Aurora αC helix is displaced relative to the rest of the Aurora structure. The binding is largely composed of hydrophobic interactions,

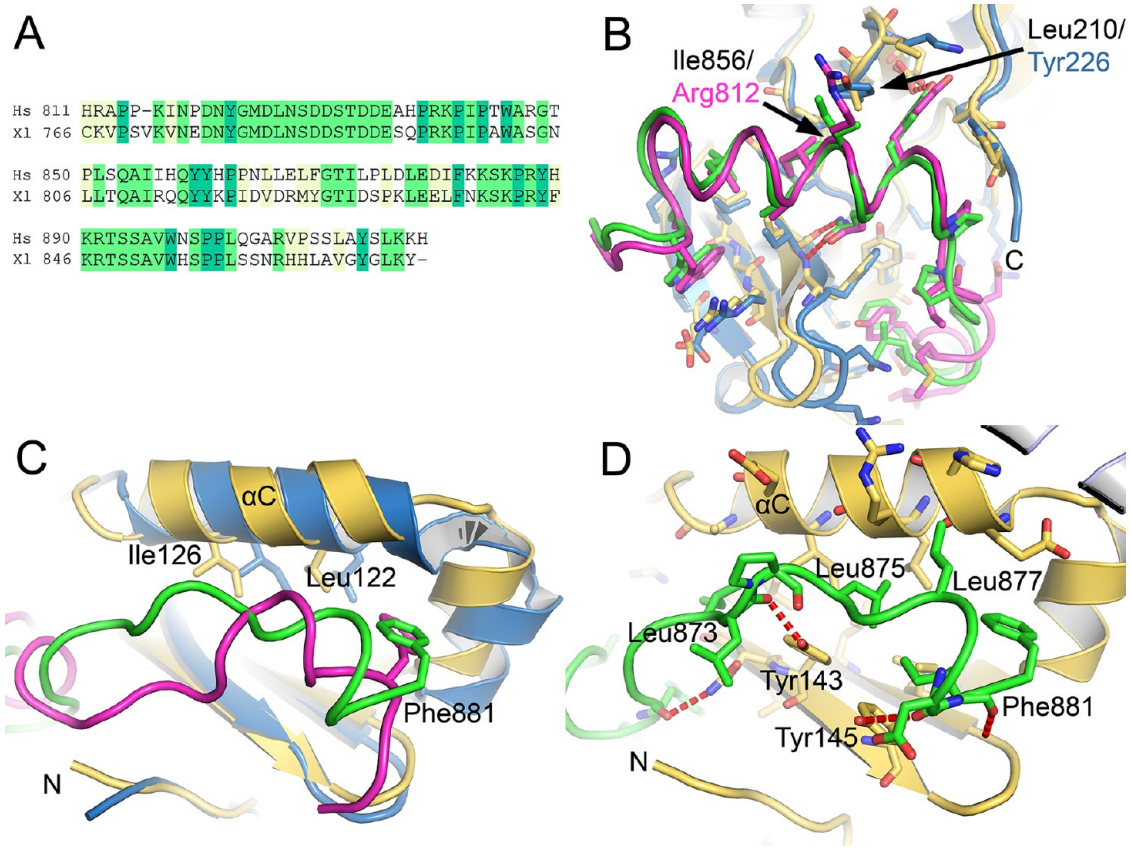

Figure 5. Interface between Aurora B kinase and INCENP. (A) Sequence alignment of human and *X. laevis* INCENP over the C-terminal IN-box region. (B) Comparison of human and *X. laevis* Aurora B:INCENP binding at site 1 (residues 842−863 of human INCENP) showing the mostly conserved interactions, with two exceptions highlighted. The *X. laevis* Aurora B and INCENP are colored blue and purple, respectively (*X. laevis* coordinates were taken from PDB ID 2BFX[8]). (C) Comparison of human and *X. laevis* Aurora B:INCENP binding at site 2 (residues 868−881 of human INCENP) showing the mostly nonconserved binding conformation, with the exception of the terminal Phe881. (D) Binding detail for site 2 of human Aurora B:INCENP.

dx.doi.org/10.1021/jm3008954 | *J. Med. Chem.* 2012, 55, 7841−7848

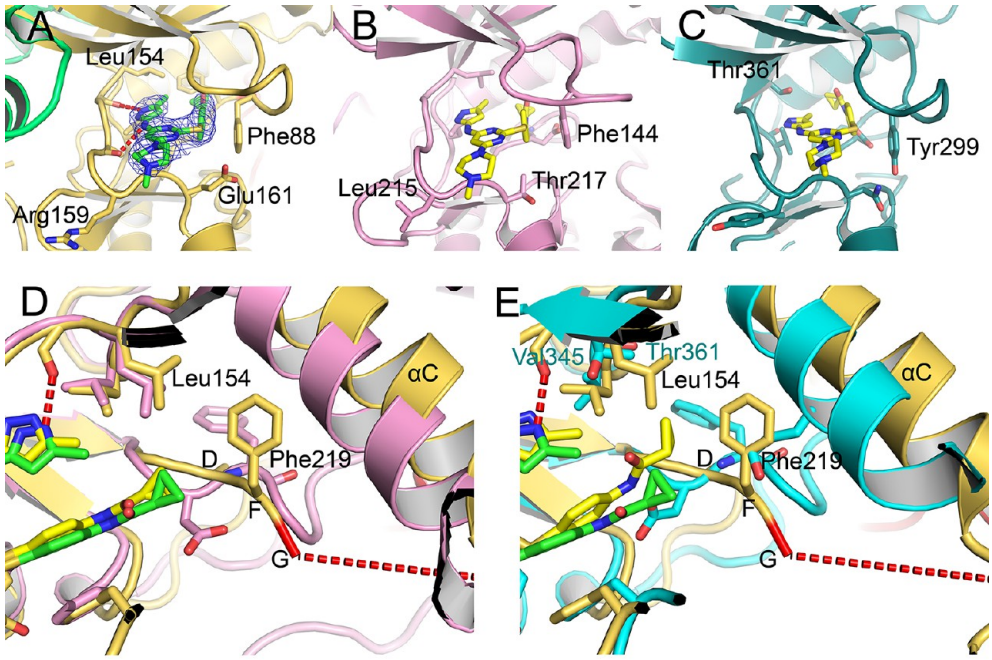

Figure 6. Comparison of binding to **1** by Aurora B, Aurora A, and ABL2. (A) Aurora B:**1**. (B) Aurora A:**1** (PDB ID: 3E5A).[13] (C) ABL2:**1** (PDB ID: 2XYN).[25] (D) Overlay of the DFG motifs of the complexes with **1** of Aurora B (in yellow) and Aurora A (in pink). (E) Overlay of the DFG motifs of the complexes with **1** of Aurora B (in yellow) and ABL2 (in blue).

particularly those around INCENP Leu875 and Leu877 (Figure 5D). Leu875 is replaced by a proline in *X. laevis* INCENP. There is also a hydrogen bond between the Aurora B Tyr145 (a histidine in *X. laevis* Aurora B) and the INCENP backbone (Figure 5D).

Aurora B:1 Has a Different αC and DFG Conformation as Compared to Aurora A and *X. laevis* Aurora B. Compound **1** binds to human Aurora B in a similar conformation to that seen in complexes with other kinases. A structure of *X. laevis* Aurora B bound to **1** is not available, so the structural comparisons of **1** binding considered here are restricted to the published structures of Aurora A:**1** (PDB ID: 3E5A)[13] and ABL2:**1** (PDB ID: 2XYN).[25] A structure of an imatinib-resistant mutant ABL1 in complex with **1** is also available.[24]

The glycine-rich loop of Aurora B is in a different conformation to that of Aurora A in the region around Phe88 (Figure 6A,B). It adopts a conformation similar to the glycine-rich loop of ABL2 when bound to **1** (Figure 6A,C), although ABL2 has Tyr299 in place of Phe88 of Aurora B. However, the most significant difference between Aurora A and Aurora B when bound to **1** is in the arrangement of the DFG motif. In Aurora A, the DFG motif is arranged with the Phe underneath the αC helix, while in Aurora B, the αC helix is moved further out from the ATP site and the DFG Phe is to the side of the helix with the Asp not well-ordered in the structure (Figure 6D). As ABL1/2 also have a similar arrangement of the DFG Phe and αC as Aurora A, Aurora B differs from all of these when bound to **1**. The movement out of αC allows more positional options for the Aurora B DFG motif and also a potentially bigger "back pocket" for inhibitor binding than in Aurora A, although due to the placement of the DFG Phe the pocket in this particular structure is slightly smaller.

Comparison of Inhibition of Human and *X. laevis* Aurora B. Comparison of the IC_{50} values for inhibition *X. laevis* Aurora B by three common Aurora kinase inhibitors with the previously published IC_{50} values for inhibition of human Aurora B by the same three inhibitors[30] shows that Aurora B from both species behaves almost identically (Table 2).

Table 2. IC_{50} Values (nM) for Inhibition of Human and *X. laevis* Aurora B by Three Aurora Kinase Inhibitors[a]

	Hs Aurora B/ INCENP	Xl Aurora B/ INCENP	Hs Aurora A/ TPX2
hesperadin	3	3	11
1	31	19	15
ZM447439	51	45	360

[a]Data on the human enzymes from Santaguida et al.[30] Binding curves can be found in the Supporting Information.

DISCUSSION

Aurora kinases have been pursued as drug targets for some time, particularly in oncology. X-ray crystal structures of Aurora A and Aurora B have been used extensively to advise medicinal chemistry efforts, either through ligand-bound structures or through their use in molecular modeling. Until now, there has not been a structure of human Aurora B kinase in the public domain, and the *X. laevis* orthologue has been used instead.

It has been predicted previously that the binding site of Aurora A:TPX2 has a smaller hydrophobic back pocket than that of Aurora B:INCENP.[19,31] Efforts to develop Aurora isoform-specific inhibitors have naturally focused on this region as well as on the differences at the entrance to the ATP binding site.[10,18−21] The Aurora B structure presented here allows direct comparison with an Aurora A structure with the same inhibitor and confirms that the hydrophobic back pocket of Aurora B is indeed larger but with the caveat that the more outward position of αC allows other conformations of the DFG motif, which may favor or disfavor particular inhibitors.

dx.doi.org/10.1021/jm3008954 | *J. Med. Chem.* 2012, 55, 7841−7848

The more outward position of αC is so far unique to human Aurora B; all of the *X. laevis* Aurora B cocrystal structures so far deposited in the PDB have a similar αC position, even with the inhibitor ZM447439, which binds much further into the hydrophobic pocket than **1** (PDB ID: 2VRX[9]), although it should be noted that the structure with ZM447439 was obtained by soaking Aurora B:INCENP crystals with the compound, and a different structure could possibly have arisen by cocrystallization. For Aurora A in the absence of TPX2, even further outward positions of αC have been observed, both with type II compounds that extend significantly into the hydrophobic pocket [e.g., PDB ID: 3DJ6 (mouse Aurora A)] and with compounds that do not (e.g., PDB ID: 2WTV or 3UNZ). In both of the structures of Aurora A in complex with TPX2 (which binds on the outside of αC), αC adopts an inward position.

The dimerization of Aurora B:INCENP that we have observed both in the crystal structure and in solution is probably the most significant factor in the different DFG motif arrangement of this complex with **1** as compared to those of Aurora A or ABL. The domain swap involves a very different conformation of the activation loop, which is most likely the cause of the different DFG position. It is unclear to what extent different inhibitors might promote or hinder dimerization. The AUC experiments showed dimerization in the absence of an inhibitor, so compound **1** was not the cause of the observed dimerization in the crystal structure. However, because the dimerization interface involves αC and is dependent on the activation loop, an inhibitor that promotes a substantially different αC position or DFG position could conceivably promote or hinder dimerization.

The variation of INCENP binding between the human and the *X. laevis* orthologues at the second site next to αC is probably a feature of the irregular backbone conformation. By contrast, at the first binding site, INCENP has an invariant α-helical backbone conformation, which inevitably leads to a more conserved binding arrangement. Whether INCENP can adopt different conformations at the second site to accommodate movements of αC during activation (or inhibition) of Aurora B is a question that has to be explored in the future.

MATERIALS AND METHODS

Cloning. DNA for residues 55−344 of the kinase domain of human AURKB (gil83776600) was PCR amplified from DNA in the Mammalian Gene Collection (IMAGE ID 2819846) and inserted into vector pNIC28-Bsa4 (which carries kanamycin resistance)[32] in-frame with an N-terminal hexahistidine purification tag and TEV protease cleavage site, by ligation-independent cloning. DNA for residues 835−903 of human INCENP (gil102467235, inner centromere protein isoform 1) was PCR amplified from INCENP cDNA and inserted into vector pGTvL1-SGC (which carries ampicillin resistance) in-frame with an N-terminal glutathione *S*-transferase purification tag and TEV protease cleavage site, also by ligation-independent cloning. These plasmids were each transformed separately into chemically competent *E. coli* BL21 (DE3) containing a plasmid for expression of rare tRNAs.

Protein Expression and Purification of Aurora B:INCENP Complex. Colonies from the transformation were used to inoculate LB media containing 34 μg/mL chloramphenicol and either 100 μg/mL ampicillin (for INCENP) or 50 μg/mL kanamycin (for Aurora B). The cultures were grown overnight in baffled shaker flasks at 37 °C with shaking. These cultures were used to inoculate TB media by adding 15 mL of culture to 1 L of TB (containing either 80 μg/mL ampicillin or 40 μg/mL kanamycin) in baffled shaker flasks. When the cultures had an OD600 of approximately 1.2, the temperature was reduced to 20 °C. After a further 25 min, protein expression was induced by addition of isopropyl β-D-1-thiogalactopyranoside to 0.5 mM. The cultures were left shaking at 20 °C overnight before the cell pellets were harvested by centrifugation. The cells were resuspended in Binding Buffer (20 mM imidazole, 200 mM NaCl, and 50 mM Tris, pH 7.8) with the addition of 0.5 mM tris(2-carboxyethyl)phosphine (TCEP) and protease inhibitor cocktail (Sigma). The resuspended cells were stored at −20 °C.

For protein purification, the resuspended cells for the Aurora B and INCENP expressions were combined and thawed together (4 L of culture of Aurora B and 6 L of culture of INCENP). The combined cells were lysed with a high-pressure homogenizer (Avestin). Polyethyleneimine was added to a concentration of 0.15%, and the lysate was centrifuged at 38000*g* for 20 min at 4 °C. The supernatant was filtered and loaded onto 10 mL of nickel-chelating resin. The resin was washed with Binding Buffer and with Binding Buffer containing 40 mM imidazole. The protein was eluted with Binding Buffer containing 250 mM imidazole, and the eluate was loaded onto a column of 10 mL of glutathione sepharose 4B resin (GE Healthcare). This resin was washed with Binding Buffer before the protein was eluted with Binding Buffer containing 10 mM reduced glutathione. The hexahistidine and GST tags were removed by overnight treatment with TEV protease at 4 °C. The digested sample was concentrated to 4 mL volume and loaded onto a Superdex75 gel filtration column (HiLoad 16/60, GE Healthcare) pre-equilibrated in GF Buffer (20 mM Hepes, pH 7.5, 200 mM NaCl, and 0.5 mM TCEP). Fractions from the gel filtration containing the desired AuroraB:INCENP complex were pooled and passed through a column of 1 mL of glutathione Sepharose 4B and then loaded onto a column of 0.7 mL of nickel-chelating resin. This resin was eluted with 5 mL each of GF Buffer containing 20, 40, 60, 80, 100, and finally 120 mM imidazole. The desired protein complex appeared in the 40−120 mM imidazole fractions. These fractions were pooled, compound **1** was added, and the sample was twice concentrated to 250 μL and then diluted to 4 mL with GF Buffer. Finally, the sample was concentrated to 200 μL volume at which the protein concentration was 6 mg/mL.

The protein identities were verified by electrospray ionization time-of-flight mass spectrometry (Agilent LC/MSD). The observed mass of Aurora B showed between 1 and 4 phosphorylations.

Crystallization and Data Collection. The AuroraB:INCENP:**1** complex (PDB ID: 4AF3) was crystallized at 20 °C in 300 nL drops from a 2:1 ratio of AuroraB:INCENP:**1** (6 mg/mL protein) and reservoir solution (10% w/v PEG3350, 0.2 M KSCN, 10% ethylene glycol, and 0.1 M BisTrisPropane, pH 6.15). The crystals were cryoprotected in reservoir solution with 25% (v/v) ethylene glycol and flash-frozen in liquid nitrogen. X-ray diffraction data were collected at 100 K on beamline I04 at DIAMOND.

Structure Determination and Refinement. The diffraction images were processed using XDS[33] and the CCP4 suite of programs.[34,35] The structure was solved by molecular replacement using PHASER[36] with the structure of *X. laevis* Aurora B (PDB ID: 2BFX) as a search model. The structure was refined against maximum likelihood targets using restrained refinement and TLS parameters, as implemented in the program REFMAC.[37] Positive difference electron density for the INCENP protein component and the inhibitor **1** was visible in the initial maps. Iterative rounds of refinement were interspersed with manual rebuilding of the model using COOT.[38] Progress of the refinement was judged throughout by following a reduction in R_{free} (calculated from a random 5% of the data that was excluded from the refinement).

AUC. Sedimentation velocity measurements were made at 40000 rpm with a Beckman An50 Ti rotor in a Beckman XL-1 ultracentrifuge at 4 °C. The protein sample was dialyzed overnight in 20 mM Hepes, pH 7.5, 200 mM NaCl, and 0.5 mM TCEP, and the protein concentration was 1.4 mg/mL for measurements. Absorbance data (280 nm) were analyzed using SEDFIT.[39,40]

Activity Measurements. Kinase assays were performed as previously described.[15] Briefly, reaction mixes contained 50 μM ATP, 1 mM DTT, 1 mM Na_3VO_4, 5 μCi γ-[^{32}P]ATP, 1 μg of histone H3 as substrate, 1 μL of DMSO or drugs dissolved in DMSO, and the

indicated kinases. Reaction mixes were incubated for 1 h at 30 °C, quenched with SDS loading buffer, and resolved on 14% SDS-PAGE. Incorporation of ^{32}P was visualized by autoradiography. Densitometry analysis was performed using ImageJ software (National Institutes of Health). IC_{50} values were calculated from log−dose response curves using Prism 4 software (GraphPad Software, Inc.).

■ ASSOCIATED CONTENT

Supporting Information

IC_{50} curves for inhibitor binding experiments. This material is available free of charge via the Internet at http://pubs.acs.org.

Accession Codes

PDB ID: 4AF3.

■ AUTHOR INFORMATION

Corresponding Author

*Tel: +44-(0)-1865-617751. Fax: +44-(0)-1865-617575. E-mail: jon.elkins@sgc.ox.ac.uk.

Present Address

⊥David H. Koch Institute for Integrative Cancer Research at MIT, Massachusetts Institute of Technology, Cambridge, Massachusetts 02139, United States.

Notes

The authors declare no competing financial interest.

■ ACKNOWLEDGMENTS

The SGC is a registered charity (number 1097737) that receives funds from the Canadian Institutes for Health Research, the Canada Foundation for Innovation, Genome Canada, GlaxoSmithKline, Lilly Canada, the Novartis Research Foundation, Pfizer, Takeda, the Ontario Ministry of Economic Development and Innovation, and the Wellcome Trust. S.S. was supported by a fellowship from the Italian Foundation for Cancer Research.

■ REFERENCES

(1) Vader, G.; Medema, R. H.; Lens, S. M. The chromosomal passenger complex: guiding Aurora-B through mitosis. *J. Cell Biol.* **2006**, *173*, 833−837.

(2) Ruchaud, S.; Carmena, M.; Earnshaw, W. C. Chromosomal passengers: conducting cell division. *Nat. Rev. Mol. Cell Biol.* **2007**, *8*, 798−812.

(3) Vader, G.; Lens, S. M. The Aurora kinase family in cell division and cancer. *Biochim. Biophys. Acta* **2008**, *1786*, 60−72.

(4) Ruchaud, S.; Carmena, M.; Earnshaw, W. C. Chromosomal passengers: conducting cell division. *Nat. Rev. Mol. Cell Biol.* **2007**, *8*, 798−812.

(5) Cheetham, G. M. T.; Knegtel, R. M. A.; Coll, J. T.; Renwick, S. B.; Swenson, L.; Weber, P.; Lippke, J. A.; Austen, D. A. Crystal Structure of Aurora-2, an Oncogenic Serine/Threonine Kinase. *J. Biol. Chem.* **2002**, *277*, 42419−42422.

(6) Nowakowski, J.; Cronin, C. N.; McRee, D. E.; Knuth, M. W.; Nelson, C. G.; Pavletich, N. P.; Rogers, J.; Sang, B.-C.; Schelbe, D. N.; Swanson, R. V.; Thompson, D. A. Structures of the Cancer-Related Aurora-A, FAK, and EphA2 Protein Kinases from Nanovolume Crystallography. *Structure* **2002**, *10*, 1659−1667.

(7) Bayliss, R.; Sardon, T.; Vernos, I.; Conti, E. Structural Basis of Aurora-A Activation by TPX2 at the Mitotic Spindle. *Mol. Cell* **2003**, *12*, 851−862.

(8) Sessa, F.; Mapelli, M.; Ciferri, C.; Tarricone, C.; Areces, L. B.; Schneider, T. R.; Stukenberg, P. T.; Musacchio, A. Mechanism of Aurora B Activation by INCENP and Inhibition by Hesperadin. *Mol. Cell* **2005**, *18*, 379−391.

(9) Girdler, F.; Sessa, F.; Patercoli, S.; Villa, F.; Musacchio, A.; Taylor, S. Molecular basis of drug resistance in aurora kinases. *Chem. Biol.* **2008**, *15*, 552−562.

(10) Kwiatkowski, N.; Deng, X.; Wang, J.; Tan, L.; Villa, F.; Santaguida, S.; Huang, H. C.; Mitchison, T.; Musacchio, A.; Gray, N. Selective aurora kinase inhibitors identified using a taxol-induced checkpoint sensitivity screen. *ACS Chem. Biol.* **2012**, *7*, 185−196.

(11) D'Alise, A. M.; Amabile, G.; Iovino, M.; Di Giorgio, F. P.; Bartiromo, M.; Sessa, F.; Villa, F.; Musacchio, A.; Cortese, R. Reversine, a novel Aurora kinases inhibitor, inhibits colony formation of human acute myeloid leukemia cells. *Mol. Cancer Ther.* **2008**, *7*, 1140−1149.

(12) Andersen, C. B.; Wan, Y.; Chang, J. W.; Riggs, B.; Lee, C.; Liu, Y.; Sessa, F.; Villa, F.; Kwiatkowski, N.; Suzuki, M.; Nallan, L.; Heald, R.; Musacchio, A.; Gray, N. S. Discovery of selective aminothiazole aurora kinase inhibitors. *ACS Chem. Biol.* **2008**, *3*, 180−192.

(13) Zhao, B.; Smallwood, A.; Yang, J.; Koretke, K.; Nurse, K.; Calamari, A.; Kirkpatrick, R. B.; Lai, Z. Modulation of kinase-inhibitor interactions by auxiliary protein binding: Crystallography studies on Aurora A interactions with VX-680 and with TPX2. *Protein Sci.* **2008**, *17*, 1791−1797.

(14) Cheetham, G. M.; Charlton, P. A.; Golec, J. M.; Pollard, J. R. Structural basis for potent inhibition of the Aurora kinases and a T315I multi-drug resistant mutant form of Abl kinase by VX-680. *Cancer Lett.* **2007**, *251*, 323−329.

(15) Honda, R.; Körner, R.; Nigg, E. Exploring the Functional Interactions between Aurora B, INCENP, and Survivin in Mitosis. *Mol. Biol. Cell* **2003**, *14*, 3325−3341.

(16) Petsalaki, E.; Akoumianaki, T.; Black, E. J.; Gillespie, D. A. F.; Zachos, G. Phosphorylation at serine 331 is required for Aurora B activation. *J. Cell Biol.* **2011**, *195*, 449−466.

(17) Keen, N.; Taylor, S. Aurora-Kinase Inhibitors As Anticancer Agents. *Nat. Rev. Cancer* **2002**, *4*, 927−936.

(18) Anderson, K.; Lai, Z.; McDonald, O. B.; Stuart, J. D.; Nartey, E. N.; Hardwicke, M. A.; Newlander, K.; Dhanak, D.; Adams, J.; Patrick, D.; Copeland, R. A.; Tummino, P. J.; Yang, J. Biochemical characterization of GSK1070916, a potent and selective inhibitor of Aurora B and Aurora C kinases with an extremely long residence time1. *Biochem. J.* **2009**, *420*, 259−265.

(19) Adams, N. D.; Adams, J. L.; Burgess, J. L.; Chaudhari, A. M.; Copeland, R. A.; Donatelli, C. A.; Drewry, D. H.; Fisher, K. E.; Hamajima, T.; Hardwicke, M. A.; Huffman, W. F.; Koretke-Brown, K. K.; Lai, Z. V.; McDonald, O. B.; Nakamura, H.; Newlander, K. A.; Oleykowski, C. A.; Parrish, C. A.; Patrick, D. R.; Plant, R.; Sarpong, M. A.; Sasaki, K.; Schmidt, S. J.; Silva, D. J.; Sutton, D.; Tang, J.; Thompson, C. S.; Tummino, P. J.; Wang, J. C.; Xiang, H.; Yang, J.; Dhanak, D. Discovery of GSK1070916, a potent and selective inhibitor of Aurora B/C kinase. *J. Med. Chem.* **2010**, *53*, 3973−4001.

(20) Shimomura, T.; Hasako, S.; Nakatsuru, Y.; Mita, T.; Ichikawa, K.; Kodera, T.; Sakai, T.; Nambu, T.; Miyamoto, M.; Takahashi, I.; Miki, S.; Kawanishi, N.; Ohkubo, M.; Kotani, H.; Iwasawa, Y. MK-5108, a Highly Selective Aurora-A Kinase Inhibitor, Shows Antitumor Activity Alone and in Combination with Docetaxel. *Mol. Cancer Ther.* **2010**, *9*, 157−166.

(21) Manfredi, M. G.; Ecsedy, J. A.; Meetze, K. A.; Balani, S. K.; Burenkova, O.; Chen, W.; Galvin, K. M.; Hoar, K. M.; Huck, J. J.; LeRoy, P. J.; Ray, E. T.; Sells, T. B.; Stringer, B.; Stroud, S. G.; Vos, T. J.; Weatherhead, G. S.; Wysong, D. R.; Zhang, M.; Bolen, J. B.; Claiborne, C. F. Antitumor activity of MLN8054, an orally active small-molecule inhibitor of Aurora A kinase. *Proc. Natl. Acad. Sci. U.S.A.* **2007**, *104*, 4106−4111.

(22) Mortlock, A. A.; Foote, K. M.; Heron, N. M.; Jung, F. H.; Pasquet, G.; Lohmann, J.-J. M.; Warin, N.; Renaud, F.; De Savi, C.; Roberts, N. J.; Johnson, T.; Dousson, C. B.; Hill, G. B.; Perkins, D.; Hatter, G.; Wilkinson, R. W.; Wedge, S. R.; Heaton, S. P.; Odedra, R.; Keen, N. J.; Crafter, C.; Brown, E.; Thompson, K.; Brightwell, S.; Khatri, L.; Brady, M. C.; Kearney, S.; McKillop, D.; Rhead, S.; Parry, T.; Green, S. Discovery, Synthesis, and *in Vivo* Activity of a New Class

of Pyrazoloquinazolines as Selective Inhibitors of Aurora B Kinase. *J. Med. Chem.* **2007**, *50*, 2213−2224.
(23) Harrington, E. A.; Bebbington, D.; Moore, J.; Rasmussen, R. K.; Ajose-Adeogun, A. O.; Nakayama, T.; Graham, J. A.; Demur, C.; Hercend, T.; Diu-Hercend, A.; Su, M.; Golec, J. M.; Miller, K. M. VX-680, a potent and selective small-molecule inhibitor of the Aurora kinases, suppresses tumor growth in vivo. *Nat. Med.* **2004**, *10*, 262−267.
(24) Young, M. A.; Shah, N. P.; Chao, L. H.; Seeliger, M.; Milanov, Z. V.; Biggs, W. H., 3rd; Treiber, D. K.; Patel, H. K.; Zarrinkar, P. P.; Lockhart, D. J.; Sawyers, C. L.; Kuriyan, J. Structure of the Kinase Domain of an Imatinib-Resistant Abl Mutant in Complex with the Aurora Kinase Inhibitor VX-680. *Cancer Res.* **2006**, *66*, 1007−1014.
(25) Salah, E.; Ugochukwu, E.; Barr, A. J.; von Delft, F.; Knapp, S.; Elkins, J. M. Crystal structures of ABL-related gene (ABL2) in complex with imatinib, tozasertib (VX-680), and a type I inhibitor of the triazole carbothioamide class. *J. Med. Chem.* **2011**, *54*, 2359−2367.
(26) Oliver, A. W.; Paul, A.; Boxall, K. J.; Barrie, S. E.; Aherne, G. W.; Garrett, M. D.; Mittnacht, S.; Pearl, L. H. Trans-activation of the DNA-damage signalling protein kinase Chk2 by T-loop exchange. *EMBO J.* **2006**, *25*, 3179−3190.
(27) Pike, A. C.; Rellos, P.; Niesen, F. H.; Turnbull, A.; Oliver, A. W.; Parker, S. A.; Turk, B. E.; Pearl, L. H.; Knapp, S. Activation segment dimerization: a mechanism of kinase autophosphorylation of non-consensus sites. *EMBO J.* **2008**, *27*, 704−714.
(28) Oliver, A. W.; Knapp, S.; Pearl, L. H. Activation segment exchange: A common mechanism of kinase autophosphorylation? *Trends Biochem. Sci.* **2007**, *32*, 351−356.
(29) Brown, P. H.; Schuck, P. Macromolecular Size-and-Shape Distributions by Sedimentation Velocity Analytical Ultracentrifugation. *Biophys. J.* **2006**, *90*, 4651−4661.
(30) Santaguida, S.; Tighe, A.; D'Alise, A. M.; Taylor, S. S.; Musacchio, A. Dissecting the role of MPS1 in chromosome biorientation and the spindle checkpoint through the small molecule inhibitor reversine. *J. Cell Biol.* **2010**, *190*, 73−87.
(31) Anderson, K.; Yang, J.; Koretke, K.; Nurse, K.; Calamari, A.; Kirkpatrick, R. B.; Patrick, D.; Silva, D.; Tummino, P. J.; Copeland, R. A.; Lai, Z. Binding of TPX2 to Aurora A alters substrate and inhibitor interactions. *Biochemistry* **2007**, *46*, 10287−10295.
(32) Savitsky, P.; Bray, J.; Cooper, C. D. O.; Marsden, B. D.; Mahajan, P.; Burgess-Brown, N. A.; Gileadi, O. High-throughput production of human proteins for crystallization: The SGC experience. *J. Struct. Biol.* **2010**, *172*, 3−13.
(33) Kabsch, W. XDS. *Acta Crystallogr.* **2010**, *D66*, 125−132.
(34) Collaborative Computational Project Number 4. The CCP4 Suite: Programs for Protein Crystallography. *Acta Crystallogr.* **1994**, *D50*, 760−763.
(35) Evans, P. Scaling and assessment of data quality. *Acta Crystallogr.* **2006**, *D62*, 72−82.
(36) McCoy, A. J.; Grosse-Kunstleve, R. W.; Adams, P. D.; Winn, M. D.; Storoni, L. C.; Read, R. J. *Phaser* crystallographic software. *J. Appl. Crystallogr.* **2007**, *40*, 658−674.
(37) Murshudov, G. N.; Vagin, A. A.; Dodson, E. J. Refinement of Macromolecular Structures by the Maximum-Likelihood Method. *Acta Crystallogr.* **1997**, *D53*, 240−255.
(38) Emsley, P.; Cowtan, K. Coot: Model-building tools for molecular graphics. *Acta Crystallogr.* **2004**, *D60*, 2126−2132.
(39) Schuck, P. Size-Distribution Analysis of Macromolecules by Sedimenation Velocity Ultracentrifugation and Lamm Equation Modeling. *Biophys. J.* **2000**, *78*, 1606−1619.
(40) Schuck, P.; Perugini, M. A.; Gonzales, N. R.; Howlett, G. J.; Schubert, D. Size-Distribution Analysis of Proteins by Analytical Ultracentrifugation: Strategies and Application to Model Systems. *Biophys. J.* **2002**, *82*, 1096−1111.